Comparative analysis of crystallization behavior induced by different mineral fillers in polypropylene nanocomposites

Luciana A. Castillo[1] and Silvia E. Barbosa[2] ⓘ

Abstract

A comparative analysis of crystallization behavior induced by several mineral fillers in polypropylene nanocomposites was performed. Morphological changes and thermal properties of nanocomposites were evaluated, considering the influence of shape, crystalline morphology, and concentration of mineral particles. For this study, hydrated magnesium silicates with different particle morphologies, such as platelets (talc) and fibers (sepiolite), were used for nanocomposites. In addition, to analyze the effect of mineral crystallinity on nanocomposites, talc and sepiolite from different origin and genesis were selected. Nanocomposites were compounded and injection molded, using different filler concentration (0, 1, and 3% w/w) for each mineral particle. To evaluate the particle influence on nanocomposite crystallinity, X-ray diffraction was used to determine crystalline phases and crystal orientation, meanwhile differential scanning calorimetry was performed to obtain thermal properties. Main results revealed that talc has a higher nucleating effect on polypropylene matrix than sepiolite fibers, regardless of their origin and genesis. Meanwhile, a transcrystalline layer that surrounds the fiber surface is observed for nanocomposite containing sepiolite. Moreover, Argentinean talc induces different crystalline phases in nanocomposite with respect to Australian one, which partly influences on mechanical properties.

Keywords

Nanocomposites, talc, sepiolite, crystallization behavior, polypropylene

Introduction

Mineral nanoparticles are widely used in polymer matrix to enhance some mechanical properties, barrier resistance, flame retardancy, and electrical and optical properties, adding only a small particle concentration.[1] These improved properties are consequence of the intrinsic particles and polymer characteristics as well as of the morphological changes induced by them in the matrix. When mineral nanofillers are incorporated to a semicrystalline polymer matrix, like polypropylene (PP), final crystalline morphology is influenced not only by particle characteristics but also by nanocomposite processing.[2] Particles contribute to the orientation of polymer chains and some of them have the capability of being nucleating agents.[3,4] This peculiar feature proceeds from the specific physicochemical interactions between mineral particles and the polymer matrix

[1] Departamento de Ingeniería Química, Universidad Nacional del Sur, Av. Alem 1253, 8000, Bahía Blanca, Argentina
[2] Planta Piloto de Ingeniería Química (UNS-CONICET), Bahia Blanca, Buenos Aires, Argentina

Corresponding author:
Silvia Barbosa, Planta Piloto de Ingeniería Química (UNS-CONICET), Camino La Carrindanga km. 7, 8000 Bahia Blanca, Buenos Aires, Argentina.
Email: sbarbosa@plapiqui.edu.ar

that promote epitaxial crystallization. However, nucleating capability of these particles depends on mineral-forming processes. Since different geological mechanisms were involved in mineral occurrence, every deposit is unique with respect to chemistry and morphology of particles.[5] In this sense, intrinsic mineral characteristics mostly depend on the physicochemical conditions that prevailed during the genesis of these materials in natural environments. Particularly, talc mineral, even though its laminar morphology, can present different crystalline character (micro- and macrocrystalline), depending on its genesis. Microcrystalline talcs contain heterogeneous stack of small and irregular platelets, meanwhile macrocrystalline ones have long, well-defined, and stacked-up platelets. These morphologies determine the size of individual talc platelets which can vary from approximately 1 μm to over 100 μm.[6] Moreover, new mineral phases occurred from preexisting ones during geological talc formation, which explain the presence of associated minerals in worldwide deposits. In this sense, chemical and structural parameters of talc particles are indicative of its origin and crystallization conditions. For this reason, talc ores differ in chemical composition, morphology, associated minerals, whiteness, and other properties.

Considering the close relationship between genesis and mineral intrinsic characteristics, Castillo et al.[7] studied the influence of particle morphology on thermal and mechanical properties of PP/talc nanocomposites. They demonstrated that talc crystalline morphology has a notable effect on final nanocomposite performance since macrocrystalline talc shows a better interfacial interaction with PP than microcrystalline one. This behavior proceeds from the formation of a thicker PP crystal on macrocrystalline particles which allows supporting higher stress than microcrystalline talc-PP composites. On the other hand, the efficiency of mineral particles as nucleating agents for PP was analyzed considering talc and pyrophyllite, which correspond to the same phyllosilicate family and present similar properties.[4] It was proved that talc is an efficient filler due to its influence on thermal and mechanical behavior of PP-based composites. However, even though pyrophyllite presents a similar structure as talc, the first mineral has a lower efficiency as nucleating agent for PP matrix than talc. This finding could be explained by the presence of distortions on pyrophyllite surface that interfere chain alignment on these mineral particles.

Of particular interest is the transcrystallization behavior of PP observed on fiber-filled nanocomposites,[8] where crystals nucleation occurs along the fiber surface. In this case, crystals grow in the normal direction to fiber surface, different from the radial direction of spherulites in bulk polymer. Generally, transcrystalline layer favors interfacial adhesion between the fibers and the polymer, leading to a significant improvement in some mechanical properties, such as longitudinal ultimate strength and modulus.[9] Transcrystallization of PP nanocomposites filled with glass fibers,[10–12] carbonaceous fibers,[13,14] and natural fibers[15–18] has been widely studied. However, transcrystallization is highly dependent on surface properties and topography as well as chemical composition of fibers.[8]

PP nanocomposites have wide industrial applications, especially in automotive, construction, and packaging fields. This is possible to the beneficial combination of lightweight, high mechanical strength, good thermal resistance, and high gas barrier. Every final application has specific requirements, which must be satisfied by intrinsic characteristics and properties of nanocomposites. As a consequence, these materials must be tailored in terms of achieving the final specifications. In this sense, it is crucial to design the nanocomposite microstructure since it will determine the material properties. As it was aforementioned, fillers influence notably on crystalline morphology of PP nanocomposites. Thus, it is important to analyze the effect of several mineral fillers with different particle morphology and concentrations on nanocomposite microstructure. This allows to determine the type of crystalline phases, the amount of crystals, the occurrence of several crystalline populations, the efficiency of particle nucleating capability, and the existence of saturation phenomenon in crystal development. Despite these aspects are important on nanocomposites final properties, the influence of laminar and fibrous particles on PP morphological changes has been scarcely investigated in the literature.

The aim of this work is to analyze comparatively the crystallization behavior induced by several mineral nanofillers in PP nanocomposites. In this sense, hydrated magnesium silicates with different particle morphologies, such as talc (platelets) and sepiolite (fibers), were considered for this study. Moreover, to evaluate the influence of each mineral crystallinity, talc from Australia and Argentina (with different origin and genesis) as well as sepiolite from Spain and Argentina were used. For all chosen mineral particles, nanocomposites were compounded and injection molded, using different filler concentration (0, 1, and 3% w/w). To evaluate the influence on nanocomposite crystallinity, X-ray diffraction was used to determine crystalline phases and crystal orientation, meanwhile differential scanning calorimetry was performed to analyze the presence of crystalline populations as well as the size and perfection of PP crystals. The study of crystallization behavior induced by mineral fillers in PP nanocomposites is crucial to understand the final morphology in terms of tailoring properties according to a specific application.

Materials and methods

Materials

Commercial PP, from Petrocuyo Argentina, was used as the polymer matrix (melt flow index: 1.8 g/10 min;

Table 1. Particle size measurements of considered mineral particles.

Mineral particle	Particle size	
ST	$d_{50} = 5.73 \pm 1.75$ µm	Fiber diameter: 33 ± 14 nm
SA	$d_{50} = 5.38 \pm 2.90$ µm	Fiber diameter: 75 ± 13 nm
TA	$d_{50} = 4.53 \pm 1.65$ µm	Platelet thickness: 79 ± 16 nm
TS	$d_{50} = 5.86 \pm 3.59$ µm	Platelet thickness: 92 ± 15 nm

TA: Australian talc; TS: Argentinean talc; SA: Argentine; ST: Spain.

weight-average molecular weight (M_w): 303,000 g mol^{-1}; M_w/number-average molecular weight: 4.45). To improve the compounding with nanoparticles, PP pellets were reduced by a plastic grinder mill, obtaining particles with an average diameter of 1700 µm. Two talc samples, supplied by Dolomita S.A.I.C, with different geological genesis were used such as Australian talc (TA) with a purity degree of 98% and Argentinean talc (TS) containing up to 15% w/w of associated minerals. Also, two sepiolite samples with different geological genesis were employed: one from Spain (ST), supplied by Tolsa S.A. with high purity (98%), and the other from Argentine (SA) with up to 10% of associated minerals (mainly carbonates). The last sample is not a commercial product. Average particle size (d_{50}) as well as talc platelet thickness and fiber diameter for the chosen mineral particles are reported in Table 1.

Nanocomposites processing and characterization

Nanocomposites were compounded by melt extrusion in a Goettfert counter-rotating twin-screw extruder ($D = 30$ mm, $L/D = 25$) with a cylindrical die (1 mm) and a screw speed of 30 r/min. Barrel temperature profile from hopper to die was 170°C–190°C–200°C–210°C–220°C, and it was held constant during compounding. After extrusion, nanocomposites were cooled by passing them through a water bath and finally pelletized. For all mineral particles, nanocomposites were prepared with concentrations of 1% and 3% w/w and were named as *PP (Particle concentration) (Type of particle)*, that is, PP1TA is a nanocomposite with 1% w/w of Australian talc.

Nanocomposite specimens were prepared by injection molding in a Fluidmec 60 T machine ($D = 40$ mm, $L/D = 19$) with a dog-bone shape. Injection temperature profile from hopper to nozzle was 165°C–190°C–195°C–210°C.

Mineral morphology as well as particle dispersion and distribution in nanocomposites were studied by scanning electron microscopy (SEM) in a LEO EVO 40 XVP-EDS Oxford X-Max 50 (CONICET, Bahía Blanca) electron microscope, with a secondary electron detector. In the first case, micrographs were performed directly onto gold-coated particles. In the second one, images were taken onto several points of cryofractured gold-coated nanocomposite samples.
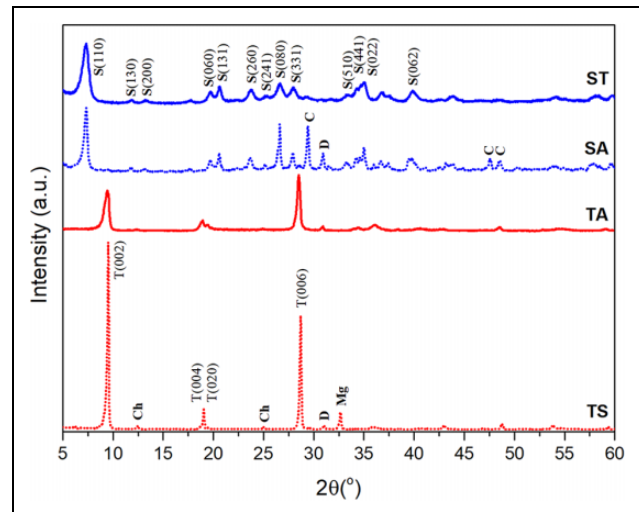

Figure 1. XRD spectra of sepiolite and talc nanoparticles. XRD: X-ray diffraction.

Thermal behavior of PP and nanocomposites injected samples was assessed by differential scanning calorimetry (DSC) under dynamic conditions using a TA Instruments Discovery DSC (CONICET, Bahía Blanca). Tests were carried out under nitrogen atmosphere at a heating/cooling rate of 10°C min^{-1}, between 30°C and 200°C. Thermal routine includes: (i) a first heating step up to 200°C reaching a complete melting, (ii) an isothermal step at 200°C for 3 min, (iii) a cooling step up to 30°C, (iv) an isothermal step at this temperature for 3 min, and (iv) a second heating step up to 200°C.

Crystalline morphology of all particles and injected samples were analyzed by X-ray diffraction (XRD). A Philips (CONICET, Bahía Blanca) PW1710 X-ray diffractometer was used, provided with a graphite curve monochromator, a copper anode, and a detector operating at 45 kV and 30 mA. For PP and nanocomposites, diffractograms were taken directly on the surface of injected specimens to analyze the induced crystalline phases by both particles and processing. Two kinds of spectra were acquired by placing the sample holder in a parallel and perpendicular direction with respect to the X-ray beam direction. In all cases, the sample holder direction matches with specimen injection direction. Five spectra for each sample in each direction were performed to verify the repeatability of the applied technique.

Results and discussion

To study the influence of sepiolite and talc on PP crystallization, firstly a structural characterization of these mineral particles was performed by XRD. Figure 1 shows diffraction patterns for sepiolite and talc nanoparticles. In sepiolite diffractograms, a strong peak is found at $2\theta = 7.32°$, which corresponds to (110) reflection. This signal is characteristic of particle minerals with a layered two-

dimensional lattice structure, and it is observed for Spanish and Argentinean sepiolite. The 2θ position of this peak coincides with that of the pristine fibrous mineral.[19–23] Particularly, (110) crystallographic plane corresponds to zeolitic pores inside sepiolite fibers.[24] In the case of Argentinean mineral (SA), main reflections are shown at 12.1, 4.5, and 3.37 Å, whose intensities revealed a notable crystalline development[25] compared to Spanish sepiolite (ST). The presence of associated minerals such as dolomite (D) and calcite (C) comes from the SA emplaced within dolomitic rock bodies.

Regarding talc, Australian and Argentinean minerals contain typical reflections of this laminar phyllosilicate such as those related to (002), (004), and (006) basal planes at $2\theta = 9.54$, 19.06, and 28.70° corresponding to 9.32, 4.68, and 3.12 Å, respectively. Argentinean talc (TS) has a lower purity degree than Australian one (TA), which can be appreciated by the number and peak intensity of associated minerals in TS spectra (Figure 1). TA showed the presence of a low-intensity peak at $2\theta = 30.92°$ associated to D, meanwhile TS contains magnesite (Mg) and chlorite (Ch), besides D. Regardless of the impurities present, TS seems to have higher crystallinity than TA which can be estimated by the maximum intensity of (002) talc reflection. To quantify the crystalline character of talc samples, a morphology index (MI) was determined considering the intensity of (004) and (020) XRD peaks.[26] This index can vary from 0 (for 100% microcrystalline samples) to 1 (for 100% macrocrystalline ones). McCarthy et al.[27] found that MI varied from 0.98 for highly macrocrystalline and platy Vermont talc to 0.45 for microcrystalline Montana ore. Particularly, MI values for talc samples considered in this work are 0.83 for TS and 0.45 for TA. These results reveal the predominant macrocrystalline morphology of TS and the microcrystalline character of TA.

Morphological characterization of sepiolite and talc particles by SEM confirms the observations previously done by XRD. Figure 2 shows micrographs of all considered mineral particles. Both sepiolite samples show the characteristic fibrous morphology, however Argentinean mineral presents a peculiar feature related to its high crystalline development. This is corroborated by the presence of long, thin, and elastic acicular particles. Moreover, nanofiber agglomerates are observed as a consequence of the collision and sticking of small fibers that previously were disaggregated from bundles. Impurities are revealed by the presence of laminar particles (marked on Figure 2) which agree with the characteristic morphology of carbonates detected by XRD (Figure 1). In the case of ST, no individual needle-like particles are distinguished, instead there are agglomerates, the sizes of which are much bigger than those observed for SA.

Even though talc is a magnesium phyllosilicate as sepiolite, its morphology is very different from the needle-shaped sepiolite particles, as it can be observed in Figure 2. Both talc samples present a laminar morphology,

regardless of their origin. However, crystalline character of TA and TS are very distinct, mainly given by the shape and size of their platelets. Microcrystalline character of TA is revealed by the presence of small, thin, and irregular platelets. Even though some rounded and pseudo-spherical aggregates are observed, they have the tendency to break and be reduced to individual small platelets at the slightest touch. On the other hand, TS is characterized by blocks having flatter and thicker particles with abrupt and well-defined borders, being characteristic aspects of macrocrystalline talc.

Structural and morphological characterization of sepiolite and talc particles revealed differences in their microscopical shape and crystalline morphology. To analyze the influence of these particles on PP nanocomposites morphology, both crystalline phases and their orientation were analyzed by X-ray diffraction. Spectra were taken in parallel and perpendicular directions with respect to X-ray beam, with sample holder always coinciding with specimen injection direction in order to assess crystal orientation in two dimensions. Figure 3 shows diffractograms, at parallel and perpendicular directions, corresponding to PP and nanocomposites containing 1% and 3% w/w of each considered mineral particles. In both directions, PP spectra contain reflections of α phase, characterized by the presence of (110), (040), (130), (111), (041), and (060) planes,[28–30] as well as a peak corresponding to β phase assigned to (300) plane. It is important to note that, although PP presents the same crystalline phases, the intensity of these reflections in parallel direction is more intense than in perpendicular one (Figure 3(a) and (b)). This result agrees with macromolecular chains orientation along the injection direction. As expected for this kind of samples, a specific crystal orientation is induced in parallel direction, coinciding with injection flow.[31]

The influence of 1% w/w incorporation of each mineral particle on PP crystalline structure can be evaluated from spectra presented in Figures 3(a) (parallel direction) and (b) (perpendicular direction). For nanocomposites containing sepiolite, mineral particle peaks are practically indistinguishable, but clear and defined α PP signals are present in both directions. On the opposite, mineral reflections in PP/talc nanocomposites are clearly distinguished even though this is not expected due to the low particle concentration. This behavior can be explained in terms of mineral morphology since sepiolite particles are fibers, meanwhile talc is composed of platelets. Despite both minerals are preferentially oriented by injection molding flow in nanocomposite specimens,[32] talc is more probable to be detected by X-ray. Talc platelets are oriented with their basal surfaces parallel to specimen one,[33] exposing a bigger surface than sepiolite fibers to X-ray beam (even for both analyzed directions). Regarding PP/sepiolite nanocomposites, all reflections of α PP present different maximum intensities, depending on the sepiolite type and particle orientation. In the perpendicular direction, ST has
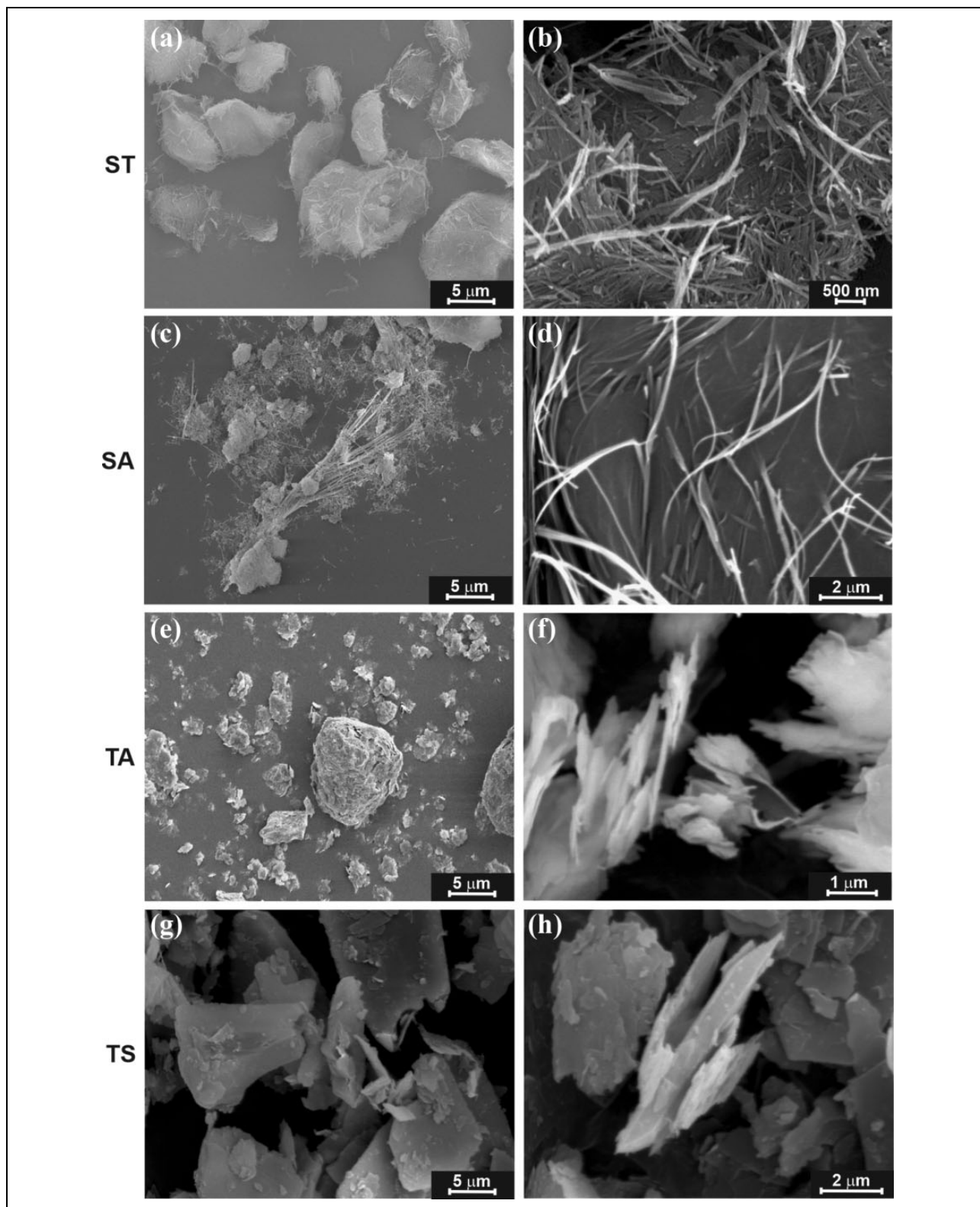
Figure 2. (a to h) SEM micrographs of sepiolite and talc nanoparticles. SEM: scanning electron microscopy.

similar peak intensity values than PP, indicating a low influence of these particles on PP crystallization. However, SA presents a higher signal maximum intensity than

ST in perpendicular direction. This behavior is in accordance with differences in sepiolite crystalline morphology and PP crystals growth from nanofiber surfaces. On the
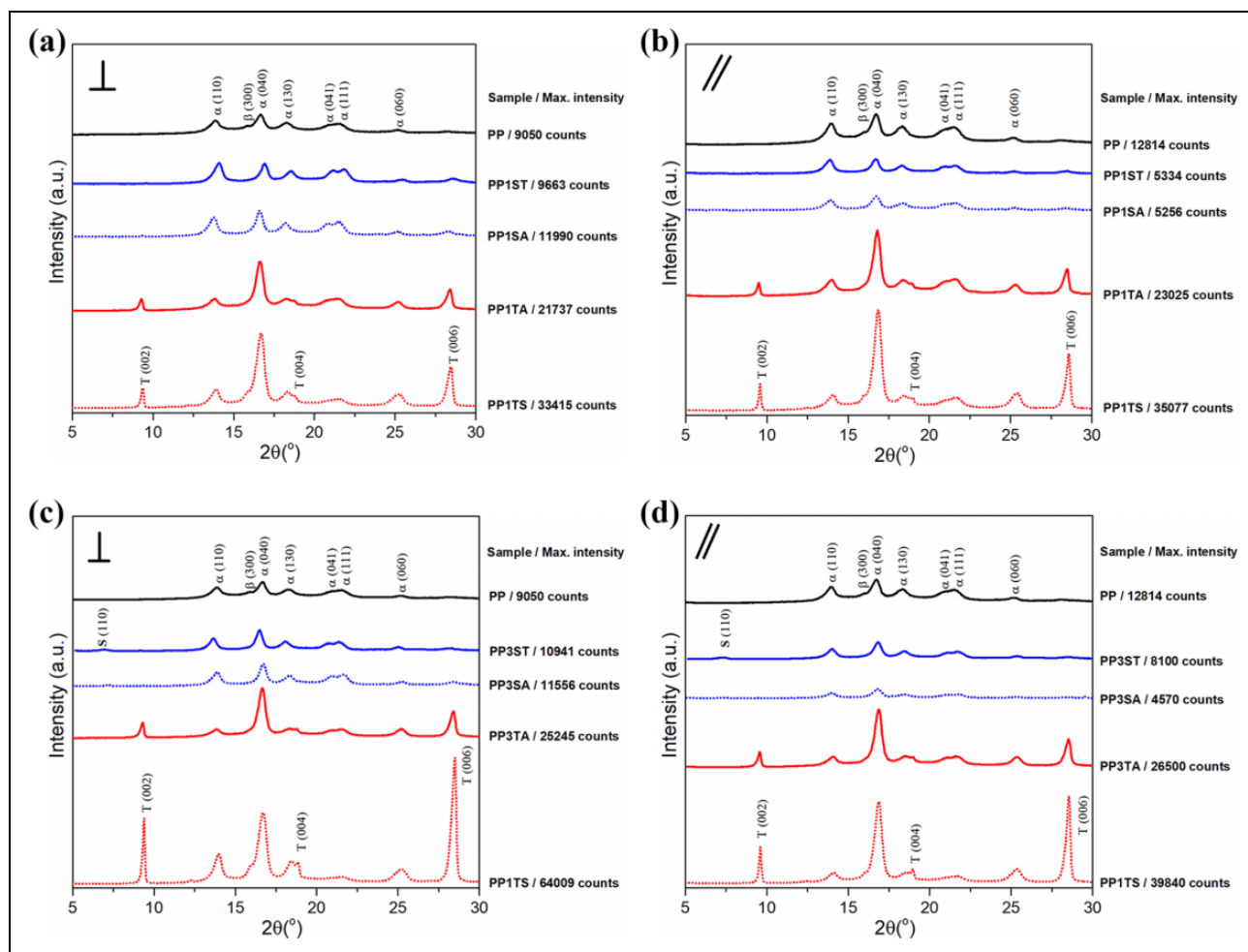
Figure 3. XRD spectra of PP and nanocomposites containing sepiolite or talc particles. (a) 1% w/w-perpendicular direction ($\perp$), (b) 1% w/w-parallel direction ($/\!/$), (c) 3% w/w-perpendicular direction ($\perp$), and (d) 3% w/w-parallel direction ($/\!/$). XRD: X-Ray diffraction; PP: polypropylene.

opposite, in parallel direction, the preferential orientation of PP crystals in sepiolite nanocomposites (given by maximum intensity comparison) is much lesser than in pure PP, independently of sepiolite type. These results are in agreement with the hypothesis of a "sort of sheathing" of PP crystals growing perpendicular to fiber axis, which is consistent with transcrystalline morphology.[34,35] On the other hand, β phase previously found in PP spectrum at approximately $2\theta = 16°$ was not detected in sepiolite nanocomposites, neither along the injection direction nor perpendicular to it. Moreover, there is no evidence of reflections at around $2\theta = 20°$ corresponding to the characteristic (117) plane for γ PP, indicating that the addition of sepiolite does not induce this crystalline phase in nanocomposites. These results are in agreement with those reported by Manchanda et al.[36] for the same nanocomposites.

The dependence of peak maximum intensities with sepiolite type and particle orientation is conserved when fiber concentration (3% w/w) is increased (Figure 3(c) and

(d)). However, some differences can be found with particle concentration since signals corresponding to sepiolite can be lightly distinguished, as expected. Moreover, sepiolite contribution to PP crystallization in perpendicular direction is similar for ST and SA, evidencing that concentration contribution is more relatively important than sepiolite type. In parallel direction, although maximum intensity in nanocomposites is lower than in PP, sepiolite type seems to induce different orientation since peak maximum intensity changed. This can be explained by the influence of crystallization morphology of sepiolite.

For nanocomposites containing 1% w/w talc, spectra in both directions (Figure 3(a) and (b), respectively) revealed the presence of well-defined mineral signals, corresponding to (002), (004), and (006) basal planes, and reflections associated to α and β PP crystals. It is important to note that, regardless of the analysis direction, the intensity of (040) reflection is much higher than (110) one. Moreover, the intensity of both reflections is much higher than those in PP and sepiolite nanocomposites
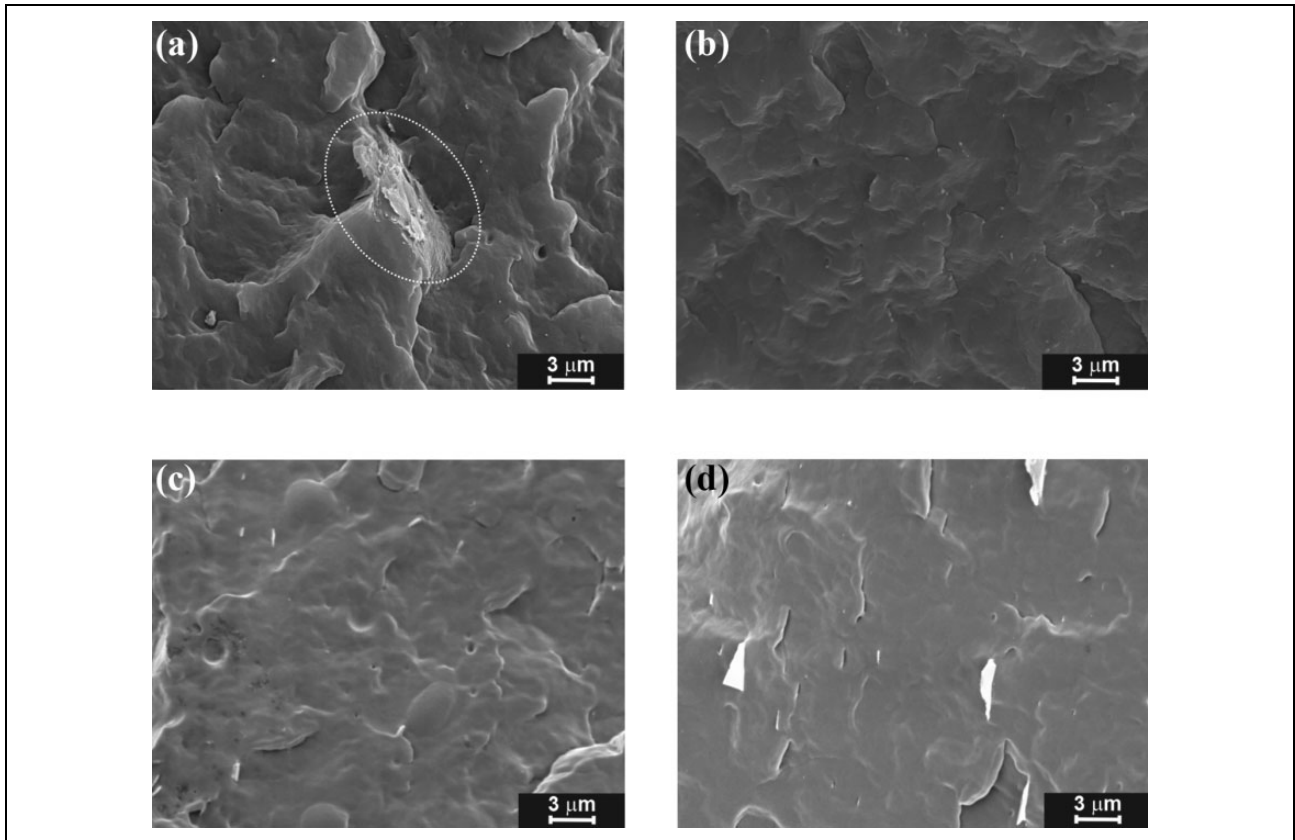
Figure 4. SEM micrographs of PP nanocomposites: (a) PP1ST, (b) PP1SA, (c) PP1TA, and (d) PP1TS. SEM: scanning electron microscopy; PP: polypropylene; TA: Australian talc; TS: Argentinean talc; SA: Argentine; ST: Spain.

spectra. This behavior proceeds from the strong nucleating capability of talc with respect to PP crystallization, as well as particle orientation aligned to the flow direction.[4,37,38] Previous works have demonstrated that there is a crystallographic matching between α PP and talc platelets, since PP tends to crystallize with a, c planes lying in a, b planes of talc, that it gives the nucleating character to this mineral.[7,39–41] Thus, oriented PP crystals showed a relative increase of (040) diffraction intensity, being a combined contribution of processing operation on chains and particles orientation as well as crystal nucleation induced by talc particles. Analyzing the influence of talc crystalline morphology, it can be observed that macrocrystalline talc (TS) allows conserving β phase previously detected in PP, different from microcrystalline talc (TA). This could be related with the size and shape of TS platelets, meanwhile TA acts as inhibitor of β PP, as it was reported previously.[42,43] It is important to highlight that α and β phases induce different mechanical properties on PP nanocomposites.[44] The presence of β phase has been reported to induce higher strength and elongation at break than α phase.[45,46] As a consequence, the induced crystalline structure by TS could bring a different mechanical performance in nanocomposites than TA.

The influence of talc concentration (3% w/w) on PP crystallization can be observed in Figures 3(c) and (d). It is observed that the induction of α and β crystalline phase is conserved (for both directions) when TS concentration is increased (Figure 3(a)). In parallel and perpendicular directions, a higher crystal orientation parallel to (040) is found in nanocomposite containing TS compared to those filled with TA. Also, a notable increase of (110) intensity for nanocomposite containing 3% w/w TS is observed in perpendicular direction. This behavior could be related to a "saturation phenomena" since the number of nucleation sites does not increase anymore, even though talc concentration continues to increase. As a consequence, particles start to impinge on each other, which avoids crystal nucleation on their surfaces. This phenomenon is reflected on crystal orientation since the amount of crystals to be oriented is lower than that at a concentration lower than the saturation one. These observations are in agreement with previous results obtained by Rybnikar.[38]

Morphological characterization of all nanocomposites is included in Figure 4. SEM micrographs of nanocomposites containing ST reveal the presence of fiber aggregates (marked in Figure 4), indicating that the dispersion was not totally effective. These aggregates have similar sizes
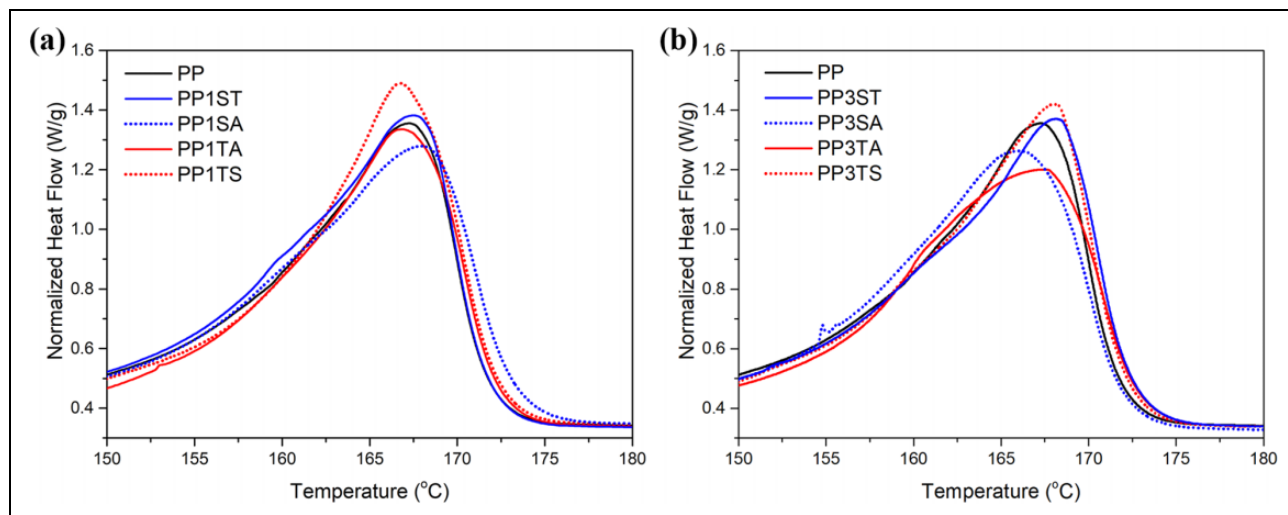
Figure 5. Thermograms corresponding to the first heating of PP and nanocomposites containing sepiolite or talc particles: (a) 1% and (b) 3% w/w. PP: polypropylene.

(4–8 μm) than those corresponding to particles in sepiolite mineral (Figure 2). However, a good matrix–fiber adhesion is evident since no fracture lines are observed at the interface and also no voids are present. The proper compatibility between PP and sepiolite was already detected by Acosta et al.[35] Even though neither ST nor SA was previously surface treated, this proper compatibility could be explained in terms of the high surface area of sepiolite fibers, as it was reported in a previous work.[24] Nanocomposites with SA particles present a morphology very different from those containing ST. As a consequence of its high crystalline development, SA appears as individual fibers which are embedded in PP, observing them as little bright pots within the matrix.

For PP/talc nanocomposites, differences in particle size are detected between nanocomposites containing TA and TS minerals, respectively. Despite both talc samples having the same initial mean particle size, TS embedded in PP matrix are bigger than TA ones. This observation proceeds from particle crystalline morphology, which is associated to geological processes that occurred during the origin of mineral deposit. Regarding TA, characteristic rounded aggregates (Figure 2) are vulnerable to be broken due to particle–particle friction and high shear fields during nanocomposite processing. For this reason, the resulting nanocomposites contain small and thin particles distributed along the polymeric matrix. On the other hand, in nanocomposites containing TS, particles nearly preserved their original size and shape. In this case, long and big platelets, corresponding to macrocrystalline morphology, are not almost altered by the processing. Another relevant characteristic to highlight is the proper talc-PP adhesion, even though no surface treatment on mineral particles was previously applied. Moreover, particle preferential orientation is observed for both PP/talc nanocomposites as a consequence of laminar morphology of

mineral particles and processing. Even though it is more evident in nanocomposites containing TS due to its macrocrystalline character, both particles are oriented in the flow direction during injection molding, as it was reported by a previous work.[47] This particle orientation is partially responsible for PP crystal orientation observed previously by XRD (Figure 3).

The study of crystallization behavior of PP nanocomposites was completed by performing a systematic thermal analysis, following the routine described in the experimental section. Results of each step of this thermal routine provide different and complementary information. In the first step, injected samples were heated to complete melting, giving information of crystalline morphology induced by particle presence and processing. The second step involves a controlled dynamic cooling which allows only to analyze the particle influence on PP crystallization. Thermal routine is completed with the analysis of melting behavior (third step) of previously cooled samples. It is important to note that, in the last two steps, processing influence cannot be detected on crystal morphology since thermal history was deleted and samples were crystallized under the same and controlled conditions.

Figure 5 shows melting thermograms corresponding to the first heating of PP and nanocomposites with 1% w/w (Figure 5(a)) and 3% w/w (Figure 5(b)) of talc and sepiolite particles. Fillers influence on crystalline morphology of injected samples is different, even for the same filler type. This induction changes with particle concentration, as it is expected and agreeing with the above XRD analysis. From Figure 5(a) it can be observed that both PP/talc nanocomposites have similar thermograms. However, Argentinean talc (TS) induces higher amount of PP crystals than Australian one (TA) because of its macrocrystalline character.[7] This tendency is similar regardless of talc concentration (Figure 5(b)). However, the influence of sepiolite particles

Table 2. Characteristic temperatures (onset, T_{peak}, and T_{offset}) determined from first and second heating for PP and nanocomposites.

	First heating		Second heating	
	T_{peak} (°C)	T_{offset} (°C)	T_{peak} (°C)	T_{offset} (°C)
PP	167.25	171.73	163.85	169.89
PP1ST	167.50	171.75	165.45	171.20
PP3ST	168.12	172.48	166.56	171.96
PP1SA	167.95	173.21	166.15	172.28
PP3SA	166.03	172.01	165.86	171.62
PP1TA	166.81	172.32	165.65	171.27
PP3TA	167.52	169.23	165.61	171.79
PP1TS	166.74	172.36	165.58	171.05
PP3TS	168.05	172.19	165.46	170.95

PP: polypropylene; T_{peak}: melting peak temperature; T_{offset}: offset temperature.

is very different on the crystallization behavior of nanocomposite injected samples. Sepiolite containing long nanofibers (SA) generates bigger and more perfect crystals than ST, as well as, than TA and TS talc (Figure 5(a)).

Table 2 lists values corresponding to melting peak temperature (T_{peak}) and offset (T_{offset}) ones for the first and second heating of all injected samples. Considering nanocomposites containing 1% w/w filler, the incorporation of SA slightly increases T_{peak}. Moreover, offset temperature, which is defined as the intersection of the tangent of peak at melting finalization with the extrapolated baseline, is also the highest for PP1SA. These observations could be explained from a higher induction of big crystals growing around the long fibers (SA), which leads to higher T_{peak} and T_{offset} values. Besides, this crystalline development is oriented perpendicular to fibers (preferentially aligned in the injection direction). For PP3SA nanocomposites, melting and offset temperatures are lower compared to those corresponding to PP1SA (Table 2). This observation indicates the presence of smaller and more imperfect crystals that could be related to a "saturation phenomenon." Since SA contains long and thin fibers but also agglomerates (Figure 2), when its concentration increases, it is more probable that particles and agglomerates get even closer. Consequently, this affects the size and shape of crystal development on sepiolite surface.

Crystallization behavior of PP and nanocomposites under controlled cooling rate is shown in Figure 6. Nanocomposites containing sepiolite do not evidence a notable difference in crystallization temperature (T_c) with respect to PP, regardless of particle morphology nor concentration. This result shows that sepiolite does not promote efficiently PP crystallization. On the opposite, talc incorporation favors the beginning of crystals development at higher temperatures than PP, for both studied particle concentrations. Moreover, talc morphology influences notably on T_c, evidencing a higher nucleating capability than sepiolite particles for PP crystallization. In this sense, nanocomposites

with Australian talc (TA) show higher T_c than those containing Argentinean one (TS). This behavior could be associated to small and irregular platelets typical of microcrystalline talc. They offer more active sites to nucleate crystals than macrocrystalline particles.

Melting behavior of PP and nanocomposites previously cooled at controlled rate is presented in Figure 7. It can be observed that T_{peak} of nanocomposites is higher than the corresponding to PP, for all considered particles and concentrations. This result indicates that the presence of bigger and more perfect crystals which are induced by particle incorporation, compared to those developed in neat PP. Filler type and morphology as well as particle concentration influence on crystalline morphology of injected samples. Nanocomposites containing sepiolite show a gradual increase of the melting onset, regardless of the particle morphology or concentration. However, two different slopes are observed in the onset behavior for PP/talc samples. These results evidenced differences in crystalline populations between nanocomposites containing sepiolite and talc particles. The gradual increasing slope on onset melting in PP/sepiolite nanocomposites revealed a broad distribution of crystallites sizes. Meanwhile, nanocomposites containing talc particles (regardless of their morphology) present a population of smaller crystals with varying size, but also a defined population of bigger crystals. This observation is evidenced for 1 and 3% w/w talc concentration, which it seems to be inherent to the laminar morphology of talc particles with respect to the acicular shape of sepiolite fibers. The influence of particle morphology on T_{peak} is more evident in PP/sepiolite than in PP/talc nanocomposites. Argentinean sepiolite (SA) presents a higher T_{peak} and T_{offset} compared to ST, which is in agreement with the bigger crystal development on long fibers. This is observed mainly at 1% w/w since the saturation phenomenon was previously evidenced at 3% w/w. With respect to nanocomposites with 1% w/w talc, T_{offset} is similar between those containing macro- and microcrystalline particles. For injected samples with 3% w/w particles, T_{offset} presents slight differences for nanocomposites having talc and sepiolite. This observation could be related to a "saturation phenomenon" where the presence of particles at a certain concentration represents a limitation since crystals start to impinge among themselves.

Conclusions

Crystallization behavior induced in PP nanocomposites by two different mineral fillers with two morphologies was analyzed. Different particle shapes such as laminar (talc) and fibrous (sepiolite) were considered for this study. Additionally, the influence of particle origin and genesis on PP crystallization was studied using microcrystalline and macrocrystalline talc and sepiolite of high and low crystalline development. Among the studied mineral particles, macrocrystalline talc was the only one that allowed conserving β phase present in PP. Talc particles induced a higher
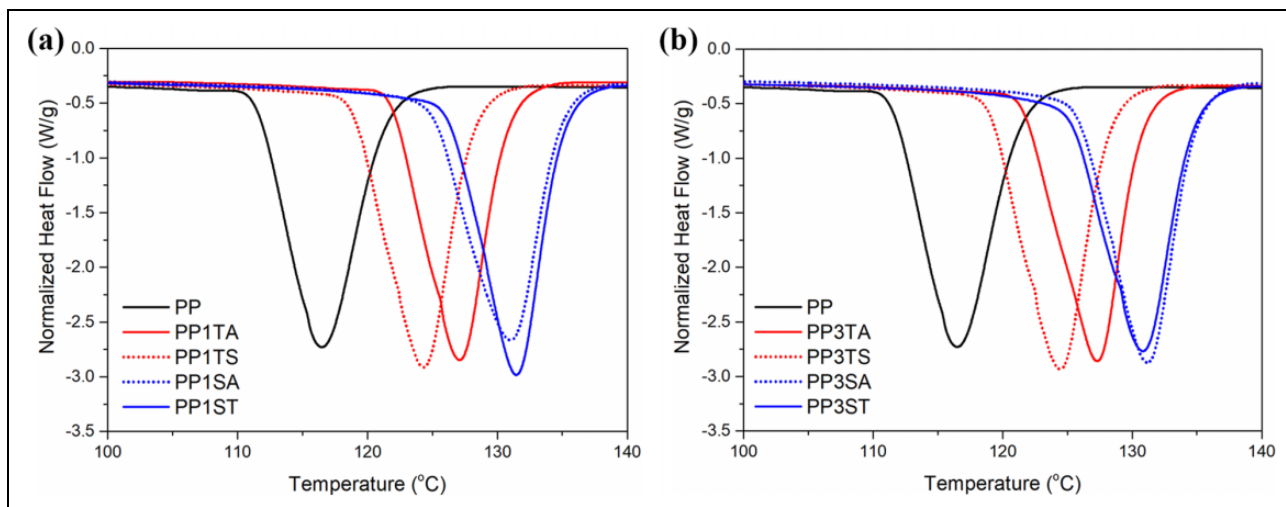
Figure 6. Thermograms corresponding to the cooling step of PP and nanocomposites containing sepiolite or talc particles: (a) 1% and (b) 3% w/w. PP: polypropylene.
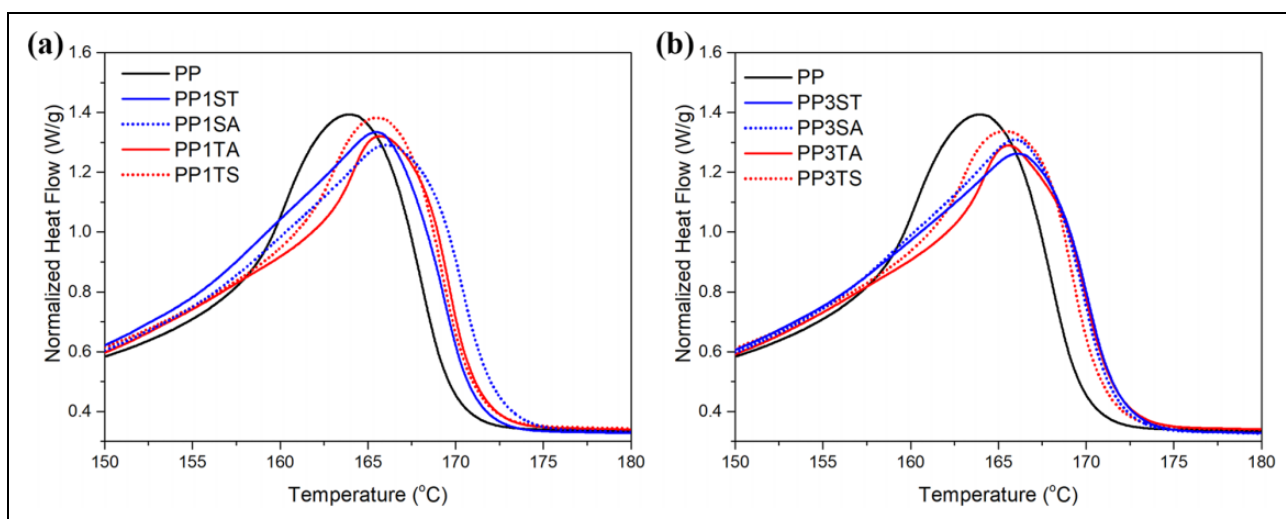

Figure 7. Thermograms corresponding to the second heating of PP and nanocomposites containing sepiolite or talc particles: (a) 1% and (b) 3% w/w. PP: polypropylene.

preferential orientation of PP crystals in nanocomposites than sepiolite as a consequence of their laminar morphology. Also, talc particles are better nucleating agents than sepiolite due to the crystallographic matching between PP and talc platelets. Sepiolite fibers mainly induced crystallization around them (transcrystallinity). The performed analysis allows to select the most appropriate particle morphology to tailor nanocomposite properties according to a specific application. This claim proceeds from the strong influence of particle morphology on several aspects of PP crystallization.

Declaration of conflicting interests

The author(s) declared no potential conflicts of interest with respect to the research, authorship, and/or publication of this article.

ORCID iD

Silvia Barbosa https://orcid.org/0000-0002-0434-0972

References

1. Fu S, Sun Z, Huang P, et al. Some basic aspects of polymer nanocomposites: a critical review. *Nano Mat Sci* 2019; 1(1): 2–30.
2. Kenig S. *Processing of polymer nanocomposites*. Munich: Hanser, 2019.

3. Avalos-Belmontes F, Ramos-deValle LF, Espinoza-Martínez AB, et al. Effect of different nucleating agents on the crystallization of ziegler-natta isotactic polypropylene. *Int J Polym Sci* 2016; 2016: Article ID 9839201.

4. Ferrage E, Martin F, Boudet A, et al. Talc as nucleating agent of polypropylene: morphology induced by lamellar particles addition and interface mineral-matrix modelization. *J Mater Sci* 2002; 37; 1561–1573.

5. Piniazkiewicz RJ, Mc Carty EF, and Genco NA. Talc. In: Carr DD (ed.) *Industrials minerals and rocks*, 6th ed. Colorado: SME Inc., 1994, pp.1049–1069.

6. de Parseval P, Moine B, Fortuné JP, et al. Fluid mineral interactions at the origin of the trimouns talc and chlorite deposit (Pyrénées, France). In: Fenoll Hach-Ali P, Torres-Ruiz J and Gervilla F (eds) *Current research in geology applied to ore deposits*. Spain: University of Granada, 1993, pp. 205–208.

7. Castillo LA, Barbosa SE, and Capiati NJ. Influence of talc morphology on the mechanical properties of talc filled polypropylene. *J Polym Res* 2013; 20(5): 152–160.

8. Quan H, Li ZM, Yang MB, et al. On transcrystallinity in semi-crystalline polymer composites. *Compos Sci Technol* 2005; 65: 999–1021.

9. Assouline E, Pohl S, Fulchiron R, et al. The kinetics of α and β transcrystallization in fibre-reinforced polypropylene. *Polymer* 2000; 41: 7843–7854.

10. Devaux E and Caze C. Evolution of the interfacial stress transfer ability between a glass fibre and a polypropylene matrix during polymer crystallization. *J Adhes Sci Technol* 2000; 14: 965–974.

11. Qin YJ, Xu YH, Zhang LY, et al. Interfacial interaction enhancement by shear-induced β-cylindrite in isotactic polypropylene/glass fiber composites. *Polymer* 2016; 100: 111–118.

12. Wang K, Guo M, Zhao DG, et al. Facilitating transcrystallization of polypropylene/glass fiber composites by imposed shear during injection molding. *Polymer* 2006; 47: 8374–8379.

13. Abdou JP, Reynolds KJ, Pfau MR, et al. Interfacial crystallization of isotactic polypropylene surrounding macroscopic carbon nanotube and graphene fibers. *Polymer* 2016; 91: 136–145.

14. Zhang SJ, Minus ML, Zhu LB, et al. Polymer transcrystallinity induced by carbon nanotubes. *Polymer* 2008; 49: 1356–1364.

15. Amash A and Zugenmaier P. Morphology and properties of isotropic and oriented samples of cellulose fibre-polypropylene composites. *Polymer* 2000; 41: 1589–1596.

16. Borysiak S. A study of transcrystallinity in polypropylene in the presence of wood irradiated with gamma rays. *J Therm Anal Calorim* 2010; 101: 439–445.

17. Joseph PV, Joseph K, Thomas S, et al. The thermal and crystallisation studies of short sisal fibre reinforced polypropylene composites. *Compos Part A Appl S* 2003; 34: 253–266.

18. Zhou M, Xu SM, Li YH, et al. Transcrystalline formation and properties of polypropylene on the surface of ramie fiber as induced by shear or dopamine modification. *Polymer* 2014; 55: 3045–3053.

19. Frost RL and Ding Z. Controlled rate thermal analysis and differential scanning calorimetry of sepiolites and palygorskites. *Thermochimi Acta* 2003; 397: 119–128.

20. Kuang W, Facey GA, Detellier C, et al. Nanostructured hybrid materials formed by sequestration of pyridine molecules in the tunnels of sepiolite. *Chem Mater* 2003; 15: 4956–4967.

21. McKeown DA, Post JE, and Etz ES. Vibrational analysis of palygorskite and sepiolite. *Clay Clay Miner* 2002; 50: 667–680.

22. Weir MR, Kuang W, Facey GA, et al. Solid-state nuclear magnetic resonance study of sepiolite and partially dehydrated sepiolite. *Clay Clay Miner* 2002; 50: 240–247.

23. Sandi G, Winans RE, Seifert S, et al. In situ SAXS studies of the structural changes of sepiolite clay and sepiolite-carbon composites with temperature. *Chem Mater* 2002; 14: 739–742.

24. Tartaglione G, Tabuani D, and Camino G. Thermal and morphological characterisation of organically modified sepiolite. *Micropor Mesopor Mat* 2008; 107: 161–168.

25. Cortelezzi CR, Marfil SA, and Maiza PJ. A sepiolite of large crystalline growth from "La Adela" mine province of Río Negro, Argentina. *Neues Jahrb Mineral Monatshefte* 1994; 4: 157–166.

26. Holland HJ and Murtagh MJ. JCPDS-international centre for diffraction data 2000 advances in X-ray. *Analysis* 2000; 42: 421–428.

27. McCarthy EF, Genco NA, and Reade EH Jr. Talc. In: Kogel JE, Trivedi NC, Barker JM and Krukowski ST (eds) *Industrial minerals and rocks*. 7th ed. Littleton, Colo: Society for Mining, Metallurgy, and Exploration, Inc., 2006, pp. 971–986.

28. Alamo RG, Kim MH, Galante MJ, et al. Structural and kinetic factors governing the formation of the γ polymorph of isotactic polypropylene. *Macromol* 1999; 32: 4050–4064.

29. Alonso M, Gonzalez A, and De Saja JA. Morphology and tensile properties of compression—moulded talc-filled polypropylene. *Plast Rub Compos Pro Appl* 1995; 24: 131–137.

30. Auriemma F and De Rosa C. Crystallization of metallocene-made isotactic polypropylene: disordered modifications intermediate between the α and γ forms. *Macromol* 2002; 35: 9057–9068.

31. Karger Kocsis J. *Polypropylene structure, blends and composites: Volume 3 composites*. Berlin: Springer Science & Business Media, 2012.

32. Wypych G. Morphology of filled systems, chapter 10. In: Wypych G (ed.) *Handbook of Fillers*. 4th ed. Toronto: ChemTec Publishing, 2016, pp. 553–569.

33. Piorkowska E and Rutledge G. *Handbook of polymer crystallization*. Hoboken: John Wiley & Sons, 2013.

34. Linares A, Morales E, Ojeda MC, et al. Interphase in polypropylene—sepiolite composites based on dynamic mechanical analysis. *Die Angew Makromol Chem* 1987; 147: 41–47.

35. Acosta JL, Morales E, Ojeda MC, et al. Effect of addition of sepiolite on the mechanical properties of glass fiber reinforced polypropylene. *Die Angew Makromol Chem* 1986; 138: 103–110.

36. Manchanda B, Kakkarakkal Kottiyath V, Kapur GS, et al. Morphological studies and thermo-mechanical behavior of polypropylene/sepiolite nanocomposites. *Polym Composite* 2015; 38: E285–E294.

37. Wang L and Sheng J. Preparation and properties of polypropylene/org-attapulgite nanocomposites. *Polymer* 2005; 46: 6243–6249.

38. Rybnikar F. Orientation in composite of polypropylene and talc. *J Appl Polym Sci* 1989; 38(8): 1479–1490.

39. Alonso M, Velasco JI, and de Saja JA. Constrained crystallization and activity of filler in surface modified talc polypropylene composites. *Eur Polym J* 1997; 33: 255–262.

40. Fujiyama M and Wakino T. Crystal orientation in injection molding of talc-filled polypropylene. *J Appl Polym Sci* 1991; 42: 9–20.

41. Radhakrishnan S, Kane K, Kadu A, et al. Structure development in processing of polypropylene films with additives. *J Appl Polym Sci* 1995; 58: 571–577.

42. Pukánszky B, Belina K, Rockenbauer A, et al. Effect of nucleation, filler anisotropy and orientation on the properties of PP composites. *Composites* 1994; 25: 205–214.

43. Zilhif AM and Ragosta G. Mechanical properties of talc-polypropylene composites. *Mater Lett* 1991; 11: 368–372.

44. Tordjeman P, Robert C, Marin G, et al. The effect of α, β crystalline structure on the mechanical properties of polypropylene. *Eur Phys J* 2001; E4: 459–465.

45. Karger Kocsis J and Varga JJ. Effects of β-α transformation on the static and dynamic tensile behavior of isotactic polypropylene. *J Appl Polym Sci* 1996; 92: 291–300.

46. Tjong SC, Shen SJ, and Li RK. Morphological behaviour and instrumented dart impact properties of β-crystalline-phase polypropylene. *Polymer* 1996; 37: 2309–2316.

47. Velasco Perero J. *Fractura de Compuestos Polipropileno-Talco*. PhD Thesis, Universitat Politècnica De Catalunya, Spain, 1996.